Japanese Journal of Applied Physics

The Japan Society of Applied Physics

RAPID COMMUNICATION

High-quality, room-temperature, surface-activated bonding of GaInAsP/InP membrane structure on silicon

To cite this article: Weicheng Fang *et al* 2020 *Jpn. J. Appl. Phys.* **59** 060905

View the article online for updates and enhancements.

This content was downloaded from IP address 131.112.125.217 on 31/07/2020 at 20:55

Japanese Journal of Applied Physics **59**, 060905 (2020) **RAPID COMMUNICATION**
https://doi.org/10.35848/1347-4065/ab958a

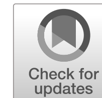

High-quality, room-temperature, surface-activated bonding of GaInAsP/InP membrane structure on silicon

Weicheng Fang[1*], Naoki Takahashi[1], Yoshitaka Ohiso[1], Tomohiro Amemiya[1,2], and Nobuhiko Nishiyama[1,2]

[1]Department of Electrical and Electronic Engineering, Tokyo Institute of Technology, O-okayama, Meguro, Tokyo 152-8552, Japan
[2]Institute of Innovative Research (IIR), Tokyo Institute of technology, O-okayama, Meguro, Tokyo 152-8552, Japan

[*]E-mail: fang.w.aa@m.titech.ac.jp

Received May 7, 2020; revised May 18, 2020; accepted May 20, 2020; published online June 4, 2020

Room-temperature surface-activated bonding (SAB) is a promising technology in large-scale hybrid photonic integration. To realize a membrane laser with low thermal resistance on Si without benzocyclobutene (BCB) bonding, a GaInAsP/InP membrane structure with a five-quantum-well active layer was bonded on Si successfully using SAB assisted by a thin a-Si film. The bonding strength reached a measurement limitation strength of 2.47 MPa for a 2 inch wafer with a thin 8.2 nm a-Si bonding layer without any annealing process for bonding. Over 90% of the bonding area, uniform photoluminescence intensity, and a well-maintained quantum-well structure were achieved after the InP-substrate removal.
© 2020 The Japan Society of Applied Physics

With the minimization of transistors, Joule heat and signal delay will prove to be challenges that cannot be ignored in large-scale integrated circuits (LSIs).[1,2] To address these challenges, one promising candidate is optical interconnection that can replace copper electrical global wiring in Si-LSIs.[3] To this end, three-dimensional integration of photonic devices on Si substrates using divinylsiloxane–benzocyclobutene (DSV-BCB)[4–6] and direct bonding[7–9] have been reported. Our group has also investigated a GaInAsP/InP membrane laser, which has very thin III–V core active layers sandwiched by low-index materials, such as SiO_2 for low threshold current operation, bonded on Si by BCB.[10–12] However, BCB has very low thermal conductivity, which makes high-temperature operation of a membrane laser difficult due to high thermal resistance. Based on our simulation using the finite element method, the thermal resistance can be reduced to less than half (from 5200 to 2600 K W^{-1}) if the thickness of BCB is reduced from 2 μm, in our previous works,[11] to 0 μm. Therefore, using direct bonding instead of BCB bonding is necessary.

Conventional direct bonding, such as hydrophilic bonding and plasma-activated bonding, requires high-temperature annealing to enhance the bonding strength,[13] thereby causing thermal stress to the bonded wafer, as well as a long processing time due to the long cooling time. Additionally, the annealing process results in a longer processing time. Therefore, room-temperature, surface-activated bonding (SAB) using fast atom beam (FAB) irradiation is attractive for the integration of III–V optical devices to a Si substrate.[14–15] Many demonstrations were reported for metal/metal bonding and Si/InP[16] bonding, by means of SAB; however, bonding of oxide materials, such as SiO_2, is known to be difficult.[17] The reason for this is assumed to be that the surface becomes inactive immediately after being activated by an FAB due to the ease of atomic reconstruction.[18] To overcome this, recently, direct bonding using a Si nanofilm was demonstrated.[18–19] However, the effects on optical properties have not been reported yet.

In this paper, we report, for the first time, on the bonding properties (including optical properties after bonding) of a GaInAsP/InP membrane structure bonded on a Si substrate using room-temperature SAB based on Ar-FAB assisted by a Si nanofilm.

Figure 1 shows the fabrication process of the GaInAsP/InP membrane structure. First, a III–V wafer, which consists of a GaInAs etch-stop layer, two InP layers, and a GaInAsP core layer (optical confinement layers and 5 quantum wells) was grown by organo-metallic vapor-phase epitaxy. Then, a 500 nm SiO_2 cladding layer was deposited on the III–V wafer by plasma-enhanced chemical-vapor deposition. After the deposition, the III–V and Si wafers were introduced to a high vacuum chamber ($<1 \times 10^{-5}$ Pa). In the first step of bonding, the target Si wafer, as the sputter source, and the III–V wafer were positioned at the bottom and top of the chamber, respectively. Then, the target Si wafer was exposed to Ar-FAB irradiation [Fig. 1(a)]. Through this irradiation, a Si nanofilm was deposited on the surface of SiO_2. Then, the target Si wafer was exchanged with a new 2 inch Si wafer as a host substrate for the membrane laser. Then, only the bottom Si wafer was irradiated by Ar-FAB [Fig. 1(b)] for surface activation. Finally, two wafers were brought into contact at room-temperature [Fig. 1(c)]. It should be noted that no post annealing process, which generally requires longer than half a day including the cooling time, was required. After bonding, the InP-substrate and GaInAs etch-stop layer were selectively wet-etched by $HCl:CH_3COOH = 3:1$ and $H_2SO_4:H_2O_2:H_2O = 1:1:40$ [Fig. 1(d)].

Before performing the bonding experiments of an actual membrane structure, bonding strength measurement was carried out through a vertical tensile test using Si/SiO_2 or InP/SiO_2 and Si wafers. The sputtering time and load value, which were the parameters used in this experiment, and the conditions during the bonding process are shown in Table I (The activation conditions are based on our previous experiment in Ref. 16). Figure 2 shows the results of the bonding strength measurements. It reveals that the bonding strength increases as the sputtering time increases. The reason may be due to the impurities and natural oxide film on the surface of the Si wafer, which caused uneven deposition in the beginning of the sputtering step. Moreover, the load value has a significant impact on the bonding strength, which may enhance atomic diffusion. Under the conditions of a sputtering time of 15 min and a 500 kgf load value, an extremely strong bond strength of over 2.47 MPa, which was the measurement limit of our tensile test equipment, was obtained in the 2 inch wafer Si/SiO_2–Si bonding. In the case of InP/SiO_2–Si, conditions with the strongest bonding strength were used; however, a lower bonding strength was recorded because of the breaking of InP itself and not due to the bonding interface.

 © 2020 The Japan Society of Applied Physics

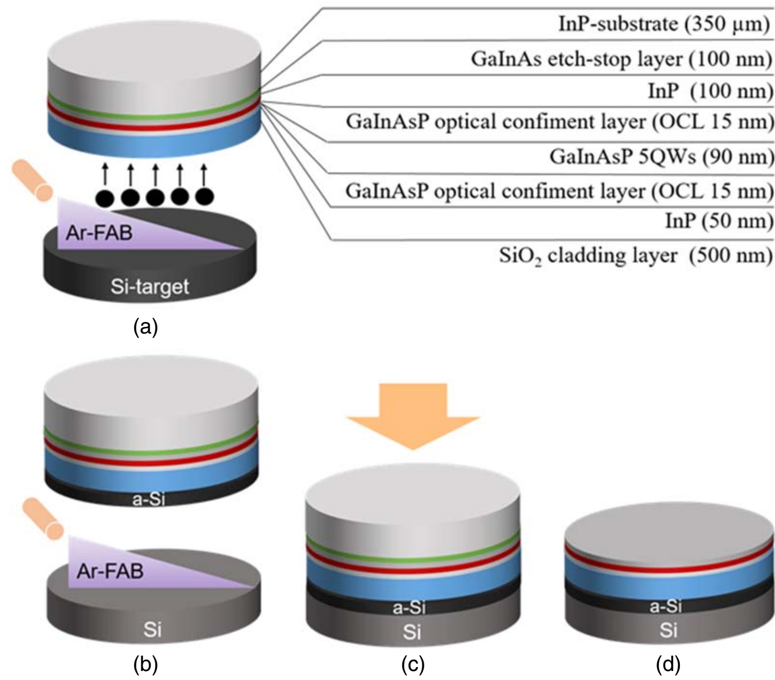

Fig. 1. (Color online) Schematic diagram of GaInAsP/InP membrane structure bonding process: (a) a-Si deposition by sputtering using Ar-FAB. (b) Surface-activated cleaning by Ar-FAB. (c) Bonding at room-temperature. (d) Removal of InP-substrate and GaInAs etch-stop layer by wet-etching.

Table I. Detailed conditions during the bonding process.

Sputtering conditions		Activation conditions		Bonding conditions	
Current	100 mA	Current	50 mA	Temperature	Room-temperature
Voltage	~1.5 kV	Voltage	~1.2 kV	Time	5 min
Time	5, 10, 15 min	Time	90 s	Load value	200 kgf, 500 kgf
Gas flow	Ar, 30 sccm	Gas flow	Ar, 30 sccm	Chamber pressure	$<10^{-5}$ Pa

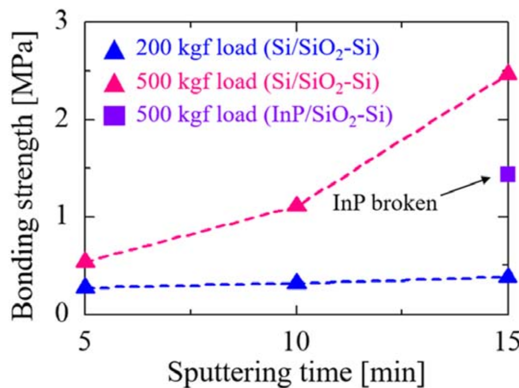

Fig. 2. (Color online) Bonding strength dependence of sputtering time and load value.

Based on the conditions described above, the GaInAsP/InP membrane structure was bonded on Si. The SiO_2/Si bonding interface was observed through a high-resolution transmission electron microscope (TEM), as shown in Fig. 3. An amorphous-like Si intermediate layer can be observed at the bonding interface (between Si-sub and SiO_2 layer) in Fig. 3(a). In Fig. 3(b), a highly magnified TEM image of the bonding interface is shown. This image indicates that the a-Si layer consists of a 5.6 nm thick upper layer and 2.6 nm thick bottom layer. To understand how these two layers are formed, the elemental composition across the SiO_2/Si bonding interface was measured by energy-dispersive X-ray spectroscopy (EDX). Peaks of Ga, C, Ti, Fe, Cu, Si, O and Ar were detected at positions *A and *B, as shown in Fig. 3(b). The composition peaks are shown in Fig. 4. The Ga peaks are due to the fabrication of the TEM observation sample using Ga focused ion beam method. The C peaks are due to the contamination caused by electron beam irradiation during TEM observation. The Ti, Fe, and Cu peaks are from the metal wafer holder (This can be avoided by using large size Si wafer as the wafer holder). At both positions, *A and *B, Si has the highest peak, and a slight amount of Ar was detected in position *B, which means that the bottom a-Si was formed by Ar-FAB irradiation. Moreover, in other works with conventional SAB, the amorphous-like layer was observed, and the thickness was determined by FAB energy.[20–21] From the combination of the TEM and EDX results, it can be inferred that the upper a-Si layer in position *A is formed by sputtering and the bottom a-Si layer in position *B is formed by cleaning irradiation.

Figure 5 shows the bonding quality of the GaInAsP/InP membrane structure bonded on Si. The bonding area after removing the InP-substrate and the GaInAs etch-stop layer by selective wet-etching are shown in Fig. 5(a). No visible voids remain at the surface of the membrane structure, and a large bonding area of over 90% was obtained successfully. The photoluminescence (PL) intensity mapping image is shown in Fig. 5(b). Almost uniform PL intensity was achieved after transforming the GaInAsP/InP membrane structure from the InP-substrate to Si substrate. These results indicate that Si

© 2020 The Japan Society of Applied Physics

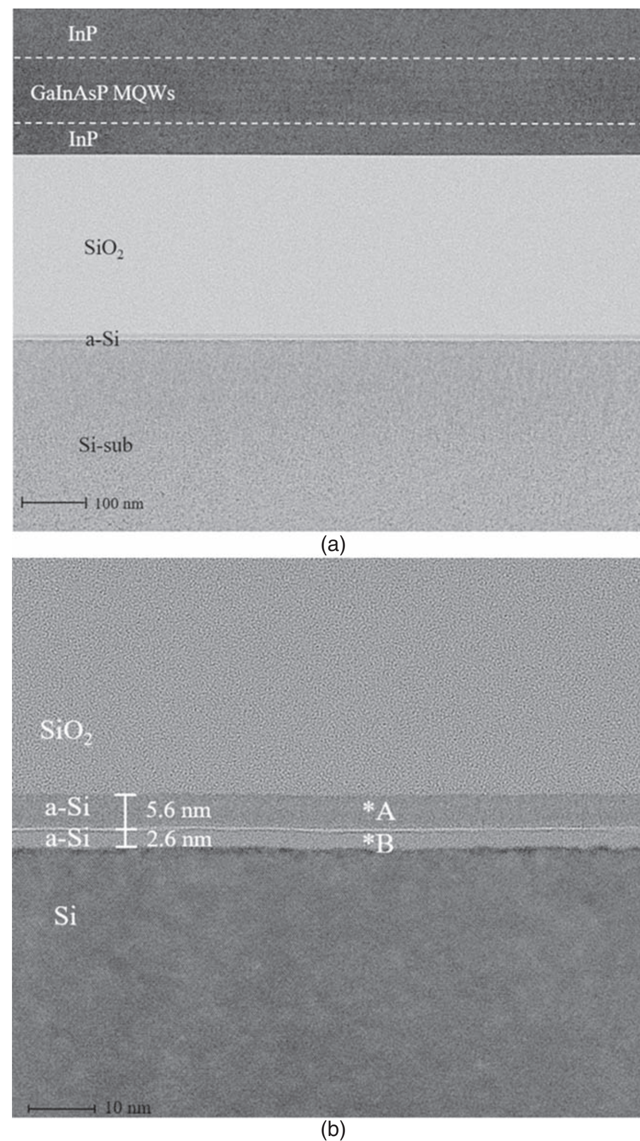

Fig. 3. Cross-sectional TEM image of SiO_2/Si bonding interface with the Ar-FAB irradiation of 15 min. (a) Low magnification and (b) high magnification. The upper a-Si layer in position *A is formed by sputtering, and the bottom a-Si layer in position *B is formed by cleaning irradiation.

nanofilm-assisted SAB has a great bonding quality after transforming the GaInAsP/InP membrane structure, which is suitable for the integration of membrane photonic devices.

To fabricate the membrane laser using the proposed bonding method, the characteristics of multi-quantum-wells (MQWs) were analyzed via PL peak wavelength measurements and X-ray diffraction (XRD) strain analysis. Figure 6(a) shows the normalized PL intensity with a peak wavelength of 1524.6 nm before bonding and 1518.8 nm after bonding and substrate removal. Furthermore, a blueshift of 5.8 nm was observed; this may be because of the occurrence of strain relaxation after the removal of the thick InP host substrate. Notably, the shoulder at approximately 1630 nm in the before bonding sample is related to the GaInAs etch-stop layer, which does not exist in the bonded wafer. Figure 6(b) shows the XRD ω-2θ scan data and fitting calculation of the as-grown epitaxial wafer and those of the bonded wafer with the removed InP-substrate. The (004) InP peak observed for the as-grown wafer and the reduced (004) InP peak observed for the bonded wafer contribute to the 350 μm thick InP-substrate and the two InP-cap layers (150 nm in total), respectively. Based on the experimental data, the relative positions of satellite peaks from "−4" to "4" are shown in the inset of Fig. 6(b), which displays an extremely slight shift, indicating that the positions of the peaks of the MQWs are well-maintained. The fitting calculation indicates that the compressive strain of the well layers in the MQWs reduced from 0.96% to 0.94%. Owing to this small strain change after bonding with 350 μm thick InP-substrate removal, it may be considered that the compressive strain relaxation results in a drop in the heavy hole level in the valence band of the quantum wells; then, the bandgap becomes slightly bigger, which is manifested as a blueshift in the PL peak wavelength.

In conclusion, a GaInAsP/InP membrane structure was bonded on a Si substrate via a-Si nanofilm-assisted SAB for membrane photonic integrated circuits. It was confirmed that the bonding strength is higher than 2.47 MPa for a 2 inch wafer without any annealing process. The bonding interface was observed via high-resolution TEM, and its elemental composition was analyzed by EDX. An approximately 8.2 nm thick a-Si thin film was included in the bonding interface, which indicates the existence of a strong SiO_2 bond. The large bonding area and uniform PL intensity

© 2020 The Japan Society of Applied Physics

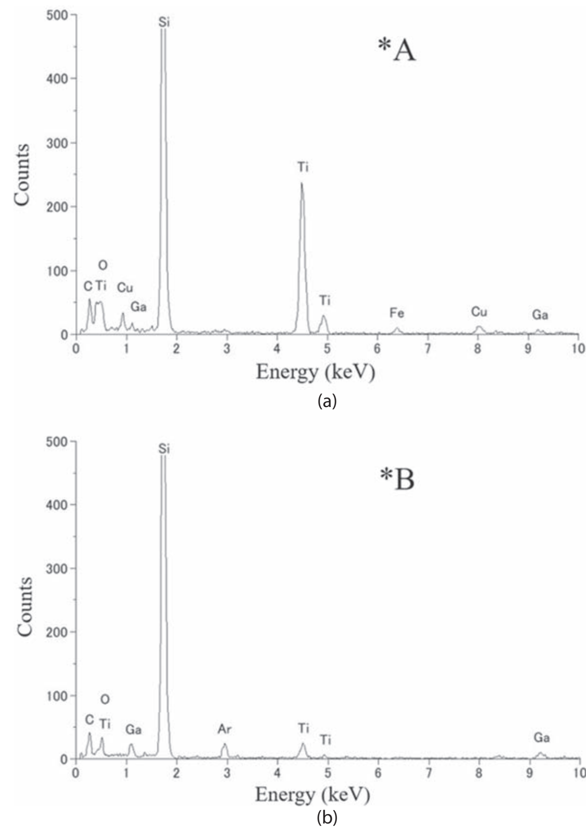

Fig. 4. EDX analysis of the intermediate layer at the bonding interface. (a) Position *A shown in Fig. 3. (b) Position *B shown in Fig. 3.

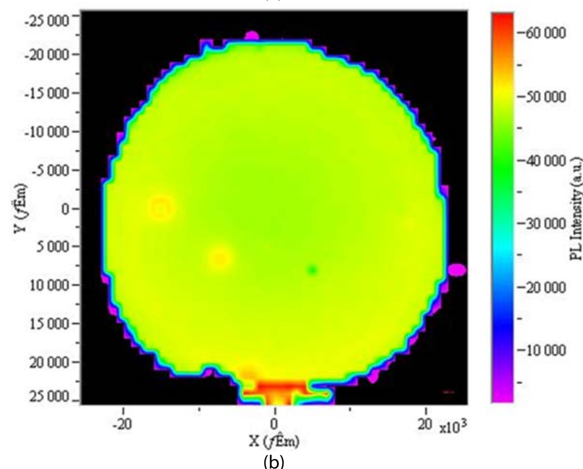

Fig. 5. (Color online) Bonding quality after removing the InP-substrate and GaInAs etch-stop layer. (a) Over 90% bonding area in 2 inch wafer bonding. (b) Uniform PL intensity mapping image after bonding.

© 2020 The Japan Society of Applied Physics

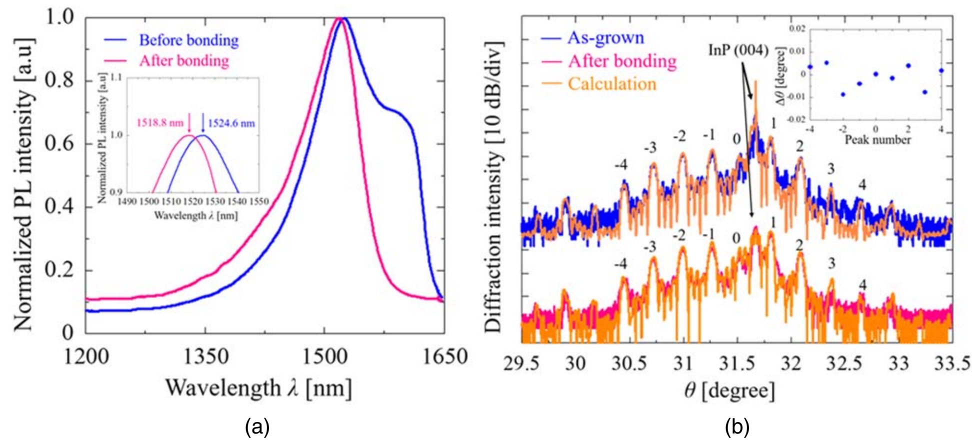

Fig. 6. (Color online) Characteristic analysis of MQWs. (a) Peak wavelength blue shifted by 5.8 nm before and after bonding. (b) XRD ω-2θ scan measurements and fitting calculation of as-grown epitaxial wafer and after bonding wafer. Inset: Relative peaks of MQWs: (−4, −3, −2, −1, 0, 1, 2, 3, 4) positions.

demonstrate that an excellent bonding quality was exhibited after the removal of the InP-substrate and the GaInAs etch-stop layer. XRD measurement shows nearly unchanged and unbroadened satellite peaks of MQWs, and the calculated data further reveal a small strain relaxation (0.02%), indicating that the crystalline structure was maintained and low-strain bonding was achieved.

Acknowledgments This work was partly supported by JST-CREST (JPMJCR15N16), JST-ACCEL (JPMJAC1603), and JSPS KAKENHI Grant Nos. (#17H03247, #19H02193).

1) P. Kapur, J. P. McVittie, and K. C. Saraswat, IEEE Trans. Electron Devices **49**, 590 (2002).
2) P. Kapur, G. Chandra, J. P. McVittie, and K. C. Saraswat, IEEE Trans. Electron Devices **49**, 598 (2002).
3) D. A. B. Miller, Proc. IEEE **97**, 1166 (2009).
4) G. Roelkens, L. Liu, D. Liang, R. Jones, A. Fang, B. Koch, and J. Bowers, Laser Photonics Rev. **4**, 751 (2010).
5) S. Stanković, R. Jones, J. Heck, M. Sysak, D. Van Thourhout, and G. Roelkens, Electrochem. Solid-State Lett. **14**, H326 (2011).
6) S. Keyvaninia, M. Muneeb, S. Stanković, P. J. Van Veldhoven, D. Van Thourhout, and G. Roelkens, Opt. Mater. Express **3**, 35 (2012).
7) A. W. Fang, B. R. Koch, R. Jones, E. Lively, D. Liang, Y. H. Kuo, and J. E. Bowers, IEEE Photonics Technol. Lett. **20**, 1667 (2008).
8) T. Plach, K. Hingerl, S. Tollabimazraehno, G. Hesser, V. Dragoi, and M. Wimplinger, J. Appl. Phys. **113**, 094905 (2013).
9) S. Matsuo, T. Fujii, K. Hasebe, K. Takeda, T. Sato, and T. Kakitsuka, Opt. Express **22**, 12139 (2014).
10) T. Hiratani, D. Inoue, T. Tomiyasu, Y. Atsumi, K. Fukuda, T. Amemiya, N. Nishiyama, and S. Arai, Appl. Phys. Express **8**, 112701 (2015).
11) T. Hiratani, D. Inoue, T. Tomiyasu, K. Fukuda, T. Amemiya, N. Nishiyama, and S. Arai, Appl. Phys. Express **10**, 032702 (2017).
12) T. Tomiyasu, T. Hiratani, D. Inoue, N. Nakamura, K. Fukuda, T. Uryu, T. Amemiya, N. Nishiyama, and S. Arai, Appl. Phys. Express **10**, 062702 (2017).
13) P. Gueguen, L. Di Cioccio, P. Gergaud, M. Rivoire, D. Scevola, M. Zussy, A. M. Charvet, L. Bally, D. Lafond, and L. Clavelier, J. Electrochem. Soc. **156**, H772 (2009).
14) T. Suga, K. Miyazawa, and Y. Yamagata, MRS Int. Meeting Adv. Mater., Mater. Res. Soc. **8**, 257 (1989).
15) H. Takagi, K. Kikuchi, R. Maeda, T. R. Chung, and T. Suga, Appl. Phys. Lett. **68**, 2222 (1996).
16) Y. Wang, K. Nagasaka, T. Mitarai, Y. Ohiso, T. Amemiya, and N. Nishiyama, Jpn. J. Appl. Phys. **59**, 052004 (2020).
17) H. Takagi, J. Utsumi, M. Takahashi, and R. Maeda, ECS Trans. **16**, 531 (2008).
18) J. Utsumi, K. Ide, and Y. Ichiyanagi, Jpn. J. Appl. Phys. **55**, 026503 (2016).
19) R. Takigawa and T. Asano, Opt. Express **26**, 24413 (2018).
20) T. Kagawa and T. Matsuoka, Appl. Phys. Lett. **69**, 3057 (1996).
21) H. Takagi, R. Maeda, N. Hosoda, and T. Suga, Jpn. J. Appl. Phys. **38**, 1589 (1999).

© 2020 The Japan Society of Applied Physics